Nuclear Instruments and Methods in Physics Research A 340 (1994) 420–426
North-Holland

NUCLEAR INSTRUMENTS & METHODS IN PHYSICS RESEARCH
Section A

Monochromator-induced glitches in EXAFS data
II. Test of the model for a pinhole sample

G.G. Li *, F. Bridges, Xun Wang

Physics Department, University of California, Santa Cruz, CA 95064, USA

Received 3 June 1993; revised form received 22 September 1993

Monochromator-induced glitches in the extended X-ray absorption fine structure (EXAFS) are studied using a pinhole sample. We have collected more detailed beam-profile data that enabled us to do a better simulation of the glitch shape. Applying the model we developed earlier, we obtain excellent agreement between the simulation and the experimental pinhole glitch. We point out that the EXAFS glitch is not caused by the crystal glitch alone, but is induced by the vertical movement of the glitch in space across the beam, as the energy is changed when the sample is non-uniform. Several methods have been suggested to minimize the glitch amplitude. Here we note that glitches can be reduced using two double-monochromators or a pair of strip array detectors for the incident and transmitted beams.

1. Introduction

The extended X-ray absorption fine structure (EXAFS) technique is a powerful tool for the study of local structure. In this technique, the absorption of X-rays is measured accurately as a function of energy, using a double crystal monochromator to achieve high energy resolution. The absorption coefficient is obtained from the ratio, $R(E)$, of the transmitted flux through the sample to the incident flux. However, the EXAFS data can be limited by the presence of spikes in the data, which we refer to as "EXAFS glitches", which are intrinsic to data collected using a double crystal monochromator in the non-dispersive mode. Crystal glitches are well known [1,2] and arise when two or more sets of Bragg planes in the monochromator crystal can simultaneously diffract X-rays at the same energy. This only happens at discrete energies (i.e. at particular angles of the monochromator crystal) and over a small range in energy. For this small energy range there is a decrease (sometimes an increase) in the diffracted intensity. For a synchrotron source, the energy of the monochromator output beam varies vertically because of the small change in incidence angle. Consequently, there is a dip in the beam profile at a position corresponding to the energy of a multiple Bragg diffraction. As the monochromator is rotated to increase the energy, this dip moves across the output beam profile. A measurement of the vertical spatial variation of the flux within a pair of slits (typically 1 mm high), shows a strong change in the spatial distribution with energy as the dip passes across the slit. This nonuniformity in the beam across a slit will couple to vertical nonuniformities in the sample leading to an EXAFS glitch that does not ratio out in $R(E)$. We have developed a model [3] to understand the formation of such glitches in EXAFS spectra which can occur even when there are no harmonics present and the detectors are very linear. In a second paper [4] we have tested this model for a sample that is tapered in the vertical direction. In this paper we consider the case of a pinhole and compare the experimental pinhole glitch with that calculated from our model. The agreement is excellent. For additional references to earlier work on EXAFS glitches and crystal glitches refer to refs. [3,4]. We emphasize that we are not addressing the origin of the crystal glitches [1,2]; they are well studied and intrinsic to the double crystal monochromator. Rather we address the question – why are glitches present in EXAFS data when simple arguments suggest that intensity variations should completely ratio out.

2. Vertical beam profiles

The experiments were carried out at SSRL on beamline 4-1 using Si(111) crystals (set 8) in the upward reflecting mode. The monochromator entrance

* Corresponding author.

0168-9002/94/$07.00 © 1994 – Elsevier Science B.V. All rights reserved
SSDI 0168-9002(93)E1050-8

slit was opened vertically to 6 mm and the detector slit (also called the exit slit) for the ionization chamber was set at 0.15 mm high by 7 mm wide. The beam profiles were recorded using energy scans from 9800 eV to 9950 eV (with 0.5 eV step) for various positions of the exit slit. The exit slit, mounted on the table, was moved vertically over a range of ~5 mm in steps of 0.2 mm. The intensities were corrected for changes in beam current. The entire incident beam profile as a function of average photon energy and vertical table position [5] is shown in Fig. 1a. Two large glitches, near 9840 eV and 9920 eV, are very prominent, while five smaller glitches, at intermediate energies, are clearly visible. More details, in the vicinity of the glitch at 9932 eV, are shown in Fig. 1b. The crystal glitch appears as a smooth dip that moves across the beam profile. The shape of the dip does not change but its vertical position shifts with energy (see Fig. 1b). There are also other small intensity variations across the beam which we do not address at this time.

The shift of the glitch with energy and with the table position is significant, as can be seen clearly in Fig. 2. Here the intensity of each scan has been normalized to 1 at 9800 eV and the scans are uniformly displaced vertically, for various table positions from 97.7 mm to 102.5 mm (table step between scans = 0.2 mm). The shifts of the glitches with table position are indicated by the dotted lines, which actually have the same energy and will be explained in the next paragraph; the shift is linear with vertical position, with a slope of about 2.4 eV/mm. The shift of the glitch with table position and energy creates significant spatial variations in the intensity of the beam across a slit. To see these changes more clearly, we have plotted in Fig. 3, the relative intensity (the intensity of a profile minus that at 9820 eV) as a function of the table position. The relative intensities are vertically displaced for various photon energies; here the energy step between profiles is 1.0 eV. In most of the region, the relative profile is quite flat. However, near a crystal glitch region, especially for the two large glitches (9840 eV and 9920 eV), the relative intensity changes rapidly with energy and table position. For example, in Fig. 3 at a table height of 100.2 mm, the slope of the intensity variation changes from zero, to positive, to zero, to negative and finally back to zero, as the energy is increased from 9830 eV to 9860 eV.

We note that the shift of the intensity dip across the beam profile as the energy is changed (as shown clearly in Fig. 2), is in a sense, not real [6,7]. The energy, E, selected by the monochromator crystals is given by Bragg's law,

$$2d(\text{Å})\sin\theta = \frac{12.4}{E(\text{keV})}. \quad (1)$$

Here d is the lattice spacing between the diffracting planes, and θ is the angle between the incident beam and these planes. For real beamlines, the incident

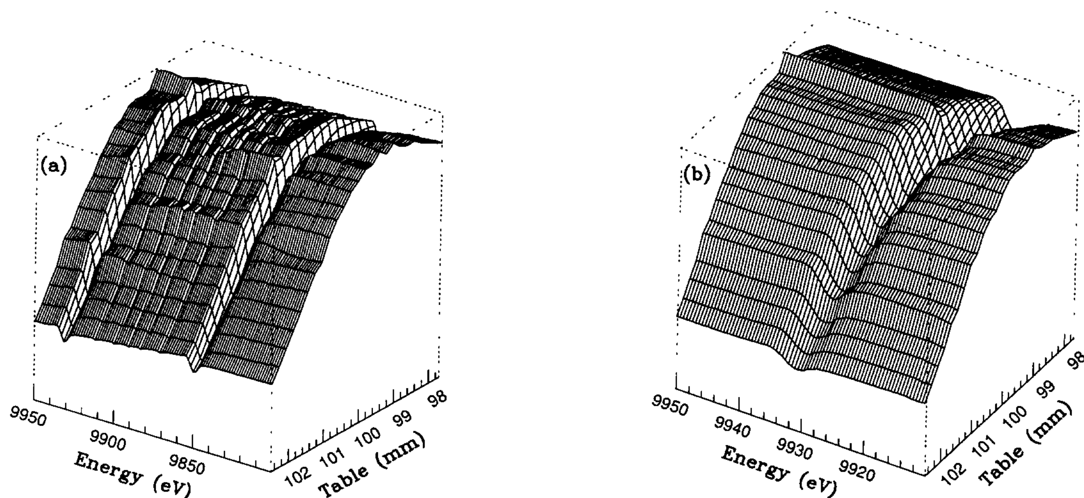

Fig. 1. Incident beam intensity from the monochromator as a function of photon energy and vertical table position. The vertical monochromator entrance slit is 6 mm and the vertical exit slit is 0.15 mm. The beam profiles were recorded using energy scans with 0.5 eV steps at various table positions. The table was moved vertically over a range of ~5 mm with a 0.2 mm step. The entire profile is shown in (a) with a 1.5 eV step in energy and a 0.2 mm step in table position. A close-up view near a glitch region is shown in (b) with a 0.5 eV step in energy and a 0.2 mm step in table position.

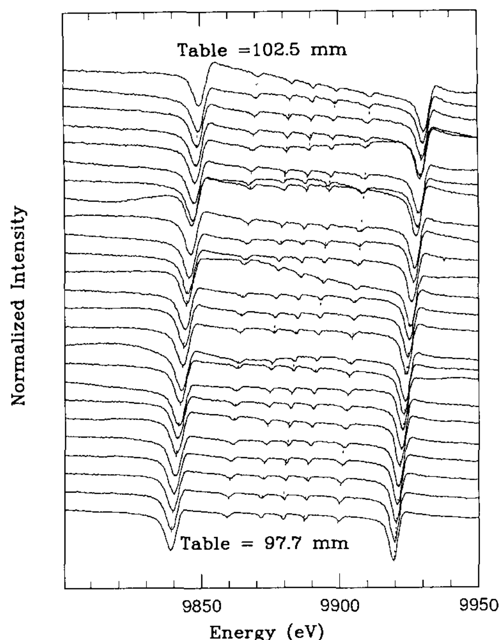

Fig. 2. Normalized incident beam intensity from the monochromator as a function of photon energy. The scans are vertically displaced for various table positions from 97.7 mm to 102.5 mm for a 0.2 mm step. The intensity of each scan has been normalized to 1 at 9800 eV. The dotted straight lines indicate the shifts of the glitch features which actually have the same energy. The slopes of the dotted lines are about 2.4 eV/mm. Thus for a fixed monochromator angle, the energy shift with the table position is -2.4 eV/mm.

radiation is not perfectly parallel. Instead, the incident beam has a small angular variation $\Delta\theta$ which will cause a variation of ΔE about the average energy given by

$$\Delta E = -E \cot \theta \Delta\theta. \tag{2}$$

In our measurements, $d = 3.136$ Å, $E \simeq 9.9$ keV, and $\Delta\theta \simeq a/L$ [5] (for an upward reflecting monochromator). Here $L \simeq 20$ m is the distance from the light source to the I_0 detector (19.54 m to the monochromator and 0.5 m between the monochromator and the I_0 detector), and a is the height of the exit slit opening. With these parameters, we calculate the energy shift rate with vertical position y to be $(\Delta E/a) = -2.4$ eV/mm, identical to the measured value, -2.4 eV/mm, obtained from Fig 2. Thus the apparent shift of the dip across the beam profile is really a consequence of the energy variation across the beam. Since double monochromators are usually used in either the upward or downward reflecting mode, the crystal glitches observed in experimental beam profiles will only move vertically, but not horizontally as the average energy is changed.

3. Theory

In transmission EXAFS measurements, the X-ray flux is measured before and after passing through a sample. The incident flux is called $I_0(E)$ and the transmitted flux is $I_t(E)$. If we define the ratio

$$R(E) = I_t(E)/I_0(E), \tag{3}$$

then the absorptance, μt, of a material is given by

$$\mu(E)t = -\ln R(E). \tag{4}$$

Here $\mu(E)$ is the absorption coefficient at photon energy E, and t is the thickness of the sample. For real situations, the thickness t and the fluxes $I_0(E)$ and $I_t(E)$ may vary with vertical position, y. Therefore, the

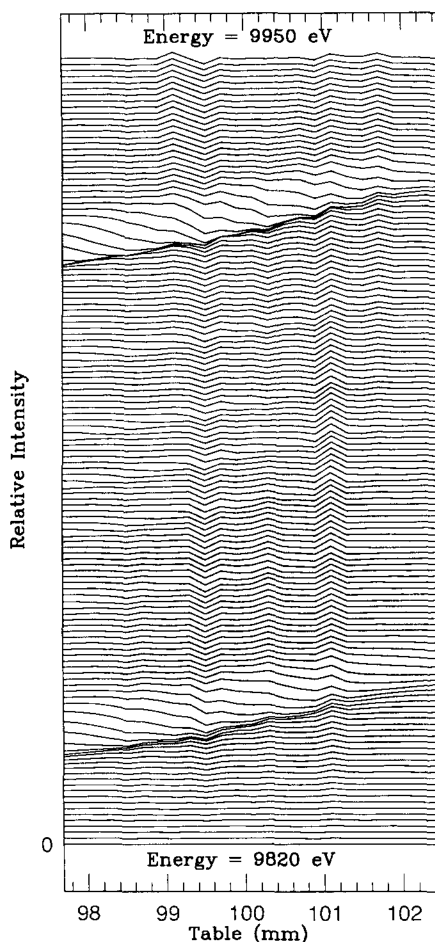

Fig. 3. The incident beam intensity distribution function relative to the profile taken at $E = 9820$ eV, as a function of the vertical table position. The relative intensities are vertically displaced for various photon energy with a 1.0 eV step.

measured fluxes are given by the following spatial averages:

$$I_0(E) = \int_{-a/2}^{a/2} F(y, E)\, dy, \tag{5}$$

$$I_t(E) = \int_{-a/2}^{a/2} F(y, E)\, e^{-\mu(E)t(y)}\, dy. \tag{6}$$

Here, $F(y, E)$ is the distribution function of the incident beam and the open detector slit is the region defined by $-a/2 \le y \le a/2$ (total slit height $= a$). If the intensity of the beam is uniform with y, then

$$\ln R(E) = \ln R_b(E) = \ln\left[\int_{-a/2}^{a/2} e^{-\mu(E)t(y)}\, dy\right] = -\mu(E)t_{eff}, \tag{7}$$

where t_{eff} is the effective thickness of the sample for absorption and R_b is the average background value of R when no glitch is present. We define the amplitude of the glitch, $A_g(E)$, by the following equation (this is slightly different from the definition used in our previous paper [4]):

$$A_g(E) = [R(E) - R_b(E)]/R_b(E) = \Delta R(E)/R_b(E). \tag{8}$$

With this definition, the glitch intensity is directly related to the fluctuations in absorptance due to the coupling of the inhomogeneity of the sample and the beam,

$$\Delta\mu(E)t = -\ln[R(E)/R_b(E)] = -\ln(1 + \Delta R(E)/R_b(E)) \simeq -\Delta R(E)/R_b(E). \tag{9}$$

For most typical cases, $|\Delta R(E)/R_b(E)| \ll 1$. The above model can be easily tested in some simple cases. As a first order approximation, we will assume that the intensity of the incident beam is a linear function of the vertical position y,

$$F(y, E) = I_o(E)(1 + \alpha(E)y)/a. \tag{10}$$

In our previous paper [4], we have tested the model for linearly tapered samples with thickness variation given by:

$$t(y) = t_0(1 + \beta y). \tag{11}$$

In that case,

$$A_g(E) = \frac{\alpha(E)}{\mu(E)t_0\beta} \times \left[1 - \frac{\mu(E)t_0\beta a}{2} \mathrm{cth}\left(\frac{\mu(E)t_0\beta a}{2}\right)\right] \simeq -\alpha(E)a^2\mu(E)t_0\beta/12. \tag{12}$$

In this paper, we will test the model for a pinhole sample (with a long horizontal slit),

$$t(y) = \begin{cases} 0 & y_p - b/2 \le y \le b/2 + y_p, \\ t_0 & \text{otherwise}. \end{cases} \tag{13}$$

Using Eqs. (5)–(9) we obtain the following result for $A_g(E)$ for the pinhole sample:

$$A_g(E) = \frac{\alpha(E)y_p(1 - e^{-\mu(E)t_0})b}{(a-b)\, e^{-\mu(E)t_0} + b} \propto \alpha(E)y_p. \tag{14}$$

Here, y_p is the pinhole position relative to the center of the detector slit ($|y_p|$ is $\le a/2$) and b is the height of the pinhole ($b \le a$). Eq. (14) shows that the EXAFS glitch from a pinhole sample changes sign when the pinhole moves across the center of the slit ($y_p = 0$) and has the highest amplitude near the edge of the slit. This prediction has been confirmed by experiment as will be described in the following section.

Eqs. (9), (12) and (14) clearly show that the fluctuation of the experimental quantity $\mu(E)t$ defined by Eq. (4) is due to the coupling of the inhomogeneities of the beam (described by $\alpha(E)$) and the sample (described by β for the tapered sample and y_p and b for the pinhole sample). Normally, $\alpha(E)$ is roughly a constant or a slowly varying function of E, thus the coupling of these nonuniformities will just add a small smooth variation to the real value of $\mu(E)t$. However, if $\alpha(E)$ varies dramatically with energy, for example, in the energy region where a crystal glitch is present, a spike will show up in the X-ray absorption data, $\mu(E)t$.

4. Glitchs from a pinhole sample: experimental measurements and model simulations

A copper foil, with an absorption length (μt) of 2.8, was prepared with a pinhole 0.13 mm high and 15 mm wide. The sample was mounted so that the pinhole was parallel to the detector slit (which was 1.3 mm high and 2.5 mm wide). The data were collected in the standard transmission mode using the same energy range and energy step as used for the profiles. In each successive scan, the sample was moved vertically so that the pinhole position, measured relative to the detector slit, was stepped from top to bottom. In addition, a trace was collected for the uniform foil to check for other nonlinearities of the detection system. No EXAFS glitches were observed which indicates that detector nonlinearities (which could couple with the beam inhomogeneity to produce EXAFS glitches [8]) are negligible in these experiments. We also collected data with the detector slit displaced horizontally away from the center of the detector by 2.0 mm to the right and to the left, respectively. These data are essentially the same as those collected with the slit centered on the ioniza-

tion detectors, which means that the region of the detectors used in these experiments is spatially uniform and horizontal inhomogeneity is negligible.

The experimental amplitude of the glitch, $A_g(E)$, was obtained using Eqs. (3) and (8); here $R_b(E)$ was approximated by a low order polynomial fit to the ratioed data, $R(E)$. The experimental data for $A_g(E)$ are shown in Fig. 4 by solid lines. The pinhole position has been defined as zero at the center of the detector slit which is at the table position of 100.2 mm. The individual traces in Fig. 4 are linearly displaced for different pinhole positions y_p for comparison purposes. We also simulated the glitchs using Eqs. (3), (5), (6), (8), (13), and the experimental profiles. The calculated results are shown in Fig. 4 as dotted lines. Both the position and the intensity of the simulated glitches agree very well with the experimental data, not only for the two big glitches, but also for the five smaller ones.

When the pinhole position, y_p, is moved from -0.50 mm below the center of the detector slit to 0.50 mm above it, the glitches obtained both from the experiments and from the simulations show a systematic change: the peak to peak height of each glitch varies from maximum to minimum and back to maximum for this range of y_p and the sign of the glitch is reversed. These changes agree very well with the simulations

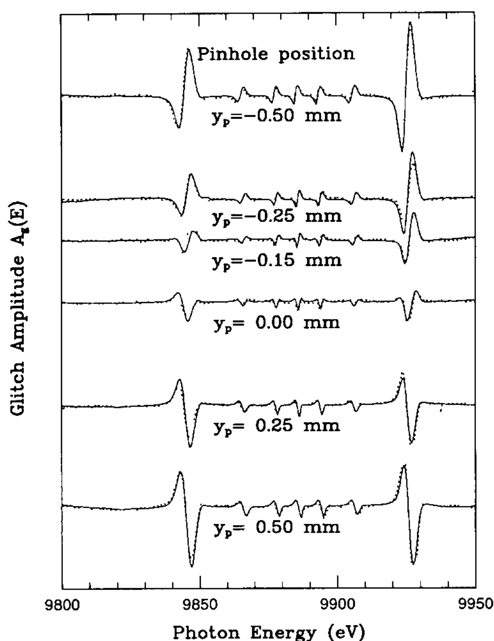

Fig. 4. Glitch amplitude, $A_g(E) = \Delta R(E)/R_b(E)$, as a function of energy for various pinhole positions relative to the center of the exit slit. The solid lines are the experimental data and the dotted lines are the simulated results. Traces for different pinhole positions are linearly displaced.

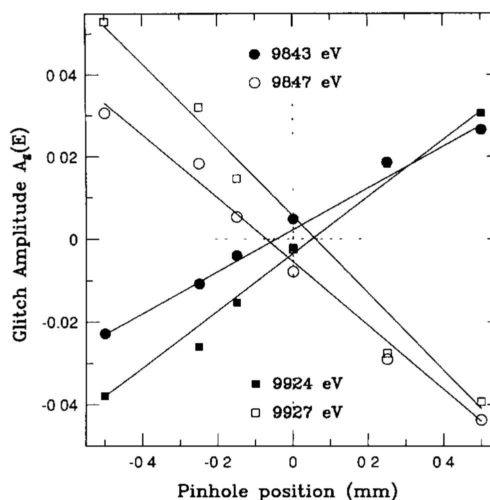

Fig. 5. Glitch amplitude, $A_g(E) = \Delta R(E)/R_b(E)$, as a function of the pinhole position for four energies which are just above and just below the central position of the two large glitches. Note that the glitch amplitude goes to zero near $y_p = 0$.

obtained using Eq. (14). To examine Eq. (14) further, we have plotted in Fig. 5 the glitch amplitude, A_g, as a function of the pinhole position for the two largest glitches. For each glitch we plot A_g at two energies, one just below the center of the glitch and the other just above it. The straight lines in Fig. 5, which are primarily a guide to the eye, follow the experimental points quite well. The slope of these straight lines changes rapidly from positive to negative within $3 \sim 4$ eV near the glitch region, which is consistent with the slope change in Fig. 3b near a table position of 100.2 mm. The intersections of the straight lines with $A_g = 0$ for 9843 eV and 9847 eV and also for 9924 eV and 9927 eV, occur near $y_p = 0$, the pinhole position for a minimum glitch amplitude. We should point out that a linear distribution function has been used for the intensity of the incident beam in Eq. (14). If a quadratic term is added to Eq. (14), the $A_g \sim y_p$ curve will vary slightly from a straight line and A_g will not be zero when y_p is zero. The small remaining glitch near $y_p = 0$ in Fig. 4 may in part be the result of a nonlinear spatial variation of the incident intensity.

5. Discussion and conclusion

If the intensity of the incident beam only changes vertically (independent of energy) or only with energy (independent of vertical position), then the crystal glitch will not show up in the ratioed EXAFS data. The EXAFS glitch shows up (assuming linear detectors and the absence of higher harmonics) if and only if the

beam intensity varies both with energy and spatial position, and a nonuniform sample is used. However, If the nonuniformities of the beam and sample are not coupled, (for example, if the beam is nonuniform vertically and the sample is nonuniform horizontally), the EXAFS glitch will still not appear. In principal there is also energy variation horizontally as a result of the horizontal angular dispersion. For the slit size and Bragg angle considered here these effects are more than three orders of magnitude smaller than those introduced by the vertical angular dispersion and hence can be neglected. This was confirmed experimentally using a horizontally tapered sample [4].

Eqs. (12) and (14) clearly show that the EXAFS glitch is due to a rapid change in the spatial variation of the incident beam intensity which is parameterized by the slope $\alpha(E)$. It is independent of the variation of the average intensity, $I_0(E)$, with photon energy (see Eq. (10)). This means that the EXAFS glitch is not caused by the crystal glitch alone, but it is induced by the vertical movement of the glitch in space across the slit, as the energy is changed. This results in a significant energy-dependent change in the spatial intensity of the incident beam. Consequently, one way to minimize the EXAFS glitch is to minimize the shift of the crystal glitch intensity dip across the slit, i.e., minimize the spatial variation in the X-ray energy across the slit. Since the energy shift across the slit, $(\Delta E/\Delta y)a$, depends on the slit height a (see Eqs. (1) add (2)), the simplest way to reduce the glitch amplitude is to reduce the slit height, as indicated in Fig. 4. In many EXAFS experiments, the signal-to-noise ratio is not statistically limited; consequently, a reduced slit height can be used with little loss in signal-to-noise. A similar conclusion was reached earlier for the tapered sample study [4]. Clearly, in an experiment for which the signal-to-noise is statistically limited by the number of photons, using a beamline with a smaller source angular divergence would be desirable since it is compatible with the use of a narrow slit.

For many beamlines, using a narrow slit of height 0.4–0.5 mm is not efficient in the use of a synchrotron X-ray source, as 80–90% of the flux is discarded (the half intensity points in the profile shown in Fig. 1 are about 4 mm apart). In transmission experiments one can make full use of the beam and still retain the advantage of a narrow slit (to minimize the glitch amplitude problem) by using two vertical arrays of slit detectors for I_0 and I_t. Consider two vertical array detectors with 10 slits, each 0.4 mm high. The two detectors must be carefully oriented so that the corresponding slits in the two detectors are aligned. Then the detector array has ten independent channels, and can collect data 5–10 times faster than a single channel. When averaging is required, which is usually the case (except for standards), such an array detector would greatly speed up data collection. Each channel would have a high energy resolution and inhomogeneities in one part of the sample (i.e. a large pinhole) would only show up in only one or two channels. We are presently developing such detectors and will report on them at a later date.

A more complicated solution for achieving higher energy resolution across the X-ray beam makes use of the fact that $\Delta E/\Delta y$ has a different sign for upward and downward reflecting double monochromators. Thus one could use two double crystal monochromators, one in the upward and the other in the downward reflecting mode (the combination is referred to as a dispersive mode), to minimize the total $\Delta E/\Delta y$. Such combinations have been used in the past ten years to improve the energy resolution in X-ray absorption measurements [9–12]. Our glitch study shows that there is an added bonus in using a pair of double monochromators; the intensity of glitches is greatly reduced.

Finally we point out that all the glitches change with pin-hole position in the same way; thus if a means is found to correct for one glitch, it should also correct the other glitches at the same time. In our previous paper we discussed minimizing the glitch amplitude by collecting two traces, one with the sample inverted about a horizontal axis. Then in a weighted sum of these two traces, the glitches will have opposite signs, and will nearly cancel. This can also be done in Fig. 4 by averaging two traces with a proper weight so that the average pin-hole position equals to zero. In this way, the amplitudes of the glitches can be reduced by 75%–95%. The above result, that all glitches vary in essentially the same way, indicates that using two traces as above, would minimize the glitch amplitude over an entire EXAFS scan.

Acknowledgements

We thank George Brown and J. Boyce for helpful discussions. The experiments were performed at the Stanford Synchrotron Radiation Laboratory (SSRL), which is operated by the U.S. Department of Energy, Division of Chemical Sciences, and by the NIH, Biomedical Resource Technology Program, Division of Research Resources. The work is supported in part by NSF grants, numbers DMR-90-04325 and DMR-92-05204.

References

[1] Z.U. Rek, G.S. Brown, and T. Troxel, in: EXAFS and Near Edge Structure 3, eds. K.O. Hodgson, B. Hedman and J.E. Penner-Hahn (Springer, New York, 1984) p. 511.

[2] K.R. Bauchspiess and E.D. Crozier, ibid., p. 514.
[3] Frank Bridges, Xun Wang and J.B. Boyce, Nucl. Instr. and Meth. A 307 (1991) 316.
[4] F. Bridges, G.G. Li and Xun Wang, Nucl. Instr. and Meth. A 320 (1992) 548, and references therein.
[5] In this and previous studies [4], the table position was defined by SSRL (before 1992) such that when the table position numerically increased the table physically moved down. This was confirmed by our collected data; the higher the energy, the lower the numerical table position. The motor control was changed so that now an increase in numerical table position corresponds to raising the table physically.
[6] J. Arthur, Rev. Sci. Instr. 60 (1989) 2062.
[7] M. Hagelstein, S. Cunis, R. Frahm and P. Rabe, Rev. Sci. Instr. 63 (1992) 911.
[8] B.R. Dobson, S.S. Hasnain, C. Morrell, D.C. Konigsberger, K. Pandya, F. Kampers, P. van Zuylen and M.J. van der Hoek, Rev. Sci. Instr. 60 (1989) 2511.
[9] D.E. Sayers, S.M. Heald, M.A. Pick, J.I. Budnick, E.A. Stern and J. Wong, Nucl. Instr. and Meth. 208 (1983) 631.
[10] S.M. Heald, Nucl. Instr. and Meth. A 246 (1986) 120; S.M. Heald, ibid. 266 (1988) 457.
[11] W.J. Trela, R.J. Bartlett, F.D. Michaud and R. Alkire, Nucl. Instr. and Meth. A 266 (1988) 234.
[12] H. Tolentino and R.D. Rodrigues, Rev. Sci. Instr. 63 (1992) 946.